



Numerical simulation of metallic honeycomb sandwich panel structures under dynamic loads

Kiumars Farhadi¹, Amir Afkar^{2*}, Majid Nouri Kamari^{2,3}

¹*Faculty of Science, Iran Polymer and Petrochemical Institute, Tehran, Iran*

²*Faculty of Electrical, Mechanical and Construction Engineering, Department of Automotive Engineering, Standard Research Institute (SRI), Karaj P. O. Box 31745-139, Iran*

³*Department of Mechanical Engineering, Shahid Rajaei Teacher Training University, Tehran, Iran*

Received 14 July 2014, Accepted 15 June 2015, Accepted 15 June 2015

**Corresponding Author E-mail: afkar@iust.ac.ir*

Abstract

In this paper, an investigation is carried out to study the dynamic mechanical response of square honeycomb core sandwich panels made from a super-austenitic stainless steel alloy using ABAQUS/Explicit. Different impulse loads on the sandwich panels are used by changing the charge weight of the explosive at a constant stand-off distance. At the lowest intensity load, significant front face bending is observed. An air blast equation is used to determine the blast loads at the front surfaces of the test panels, and these were used as inputs to finite element calculations of the dynamic response of the sandwich structure. Very good agreement is noticed between the finite element model predictions of the sandwich panel front and back face displacements and the data available in literature. It is also found that the honeycomb sandwich panels suffers significantly from smaller back face deflections than solid plates of identical mass.

Keywords: Blast loading; Finite element simulation; Impulse loads; Sandwich panels

1. Introduction

The necessity and need to protect structures against extreme dynamic loads generated by explosives, a new focus on the response of metallic structures exposed to high concentrated load, is raised. One of the promising methods is the using of sandwich panels to disperse the transferred mechanical impulse to the structure. In this way, the pressure applied on the protected structure in behind of the panel is reduced [1-3]. It is a sandwich panel consisting of a pair of thin hard metal surface and a metal honeycomb core with reinforced edges which explosive charge is exploded above it. The dynamic response of sandwich structures under impact load has been studied in several researches [4, 5]. Detailed finite element analysis conducted using all meshed geometries with square honeycomb, prismatic grooves and pyramidal truss which made of materials with specified flow strength, stiffness and sensitivity to strain rate. These studies represent the dynamic response of complicated structures. For near-field air blast the shock wave released from the explosion source to front page and reflected. Pressure of the shock wave is analyzed according the distance (the source of the explosion) and time. When the shock is applied on a rigid surface, the front of shock wave undergoes reflection (echo). This requires the forward moving air molecules comprising the shock wave to be brought to rest and further compressed inducing a reflected overpressure on the wall which is of higher magnitude than the incident overpressure [6]. An impact to the front surface of the structure resulted in its speed increasing. In the acoustic limit, the pressure pulse applied to the sample front face during this process is twice that of the free-field shock (large stand-off distances and for

weak explosions). In the near field where on-linear effects are present in the shock front, the pressure reflection coefficient can rise to a value of eight (under an ideal gas assumption). Even larger pressure reflection coefficients result when real gas effects (dissociation and ionization of the air molecules) occur in the free field shock [7].

In the near field where non-linear effects are present in the shock front, the pressure reflection coefficient passes a critical value, eight (under an ideal gas assumption).

Even when real gas effects (failure to ionize the air molecules) in free square shock occurs, it results in greater pressure reflection coefficients [7]. Deshpande and Fleck [8] called this initial phase of the blast shock–structure interaction Stage I. For an ideal blast without shock reflection, a front face of mass m_f moves at a velocity V_1 towards the back face sheet, and requires its full momentum ($m_f V_1$) at the end of stage I. For sandwich panel structures, this front face motion is strengthened by compression of the cellular core. A region of densified core is then created at the front face and this propagates at the core plastic wave speed towards the back face. This plastic wave speed V_p is obtained as:

$$V_p = \sqrt{\frac{E_t}{\bar{\rho}}} \quad (1)$$

where E_t is the tangent modulus of the material used in core of structure and $\bar{\rho}$ is its density. V_p is 500 m/s for stainless steel alloys subjected to plastic strains of around 10%. It is about a tenth of the elastic wave speed of the materials used to make the structure. Core crushing occurs at a characteristic pressure and this crushing retrofits the front plate movement and decrease the front face motion. For weak explosive shocks, it is possible to arrest the densification front within the core. The pressure that is transmitted to the support structure is controlled by the dynamic crush strength of cellular material during densification. This crush strength depends on the core density, cell topology and material properties, which are used to make the honeycomb structure [9].

For large concentrated spatial impacts, hitting transferred to the back surface sheet can be enough to bend the panels which are sealed at the edges. During this panel bending, further mechanical energy dissipation occurs by a combination of core collapse and core/face sheet stretching. In a properly designed system, the inhibitor force with the distribution of plastic are enough to arrest the motion of the panel before the loads applied to the support structure exceed design objectives, or tearing of the front face plate occurs. It is important to recognize that core crushing continues to play an important role during stage III because highly crush resistant cores maintain a larger face sheet separation and therefore higher panels bend resistance [7].

The biggest advantage of FRPs is their tailor ability. They can be more easily arranged according to the specific site conditions than other materials and so optimized for performance. FRP retrofitting can be applied quickly, is non-intrusive and provides a dramatic increase in the ability of a building to resist an explosion. Efforts to implement these blast shock wave protection concepts require a detailed understanding of the dynamic structural response and core collapse mechanisms, the development of a design science that enables preferred core topologies, core relative densities and core materials to be identified, and manufacturing approaches for the materials/topologies of interest. Recent studies indicate that a square honeycomb topology with the webs aligned perpendicular to the face sheets has the highest crush resistance [10-14]. Significant quasi-static core strength enhancements can be achieved by constructing such cores from metals with a high yield strength and tangent modulus. This causes web buckling to control the core strength and the critical strength for this buckling mode can increase by increasing the web material's tangent modulus. During dynamic loading, additional core strengthening has been predicted to occur by inertial buckling stabilization and strain rate hardening. Materials with a high strength, tangent modulus and strain hardening rate are then best suited for blast wave mitigation applications. Many austenitic and super-austenitic stainless steels have a desirable combination of these properties [15].

In protecting buildings from progressive collapse, the shear capacity of a retrofitted column shall exceed its flexural strength. This avoids the brittle shear failure and allows a more ductile flexural response. The shear capacity of RC beams may also be increased by applying externally bonded FRP. The methods include bonding strips or continuous sheets of FRP to the vertical sides of a beam, bonding FRP U-jackets around the two sides and the tension face and wrapping FRP around the whole circumference of a beam (Fig. 1).

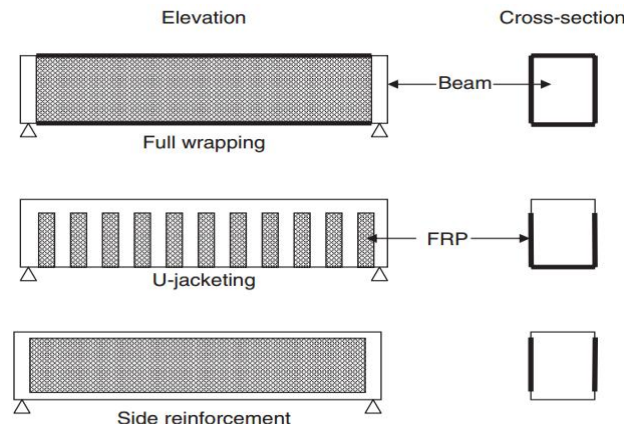


Figure 1. Shear strengthening of concrete beams with FRP

Recent cellular manufacturing developments now enable the fabrication of many cellular metal core structures from stainless steels. These include the fabrication of triangular and square honeycombs, prismatic corrugations, lattice truss structures with pyramidal, tetrahedral, three dimensional Kagome architectures, and lattice structures with hollow truss or wire mesh lay-ups. These cellular metal cores can be attached to face sheets using transient liquid phase bonding methods to create sandwich panel structures [16, 17].

In this paper numerical finite element simulations of sandwich panels under shock waves which is produced by air blast were performed using ABAQUS software to investigate the dynamic deformation sequence and the core collapse mechanisms controlling the overall response.

2. Air blasts

When an ablast occurs in air, it produces compress the surrounding air and moves them outwards with a high velocity. Their initial velocity is close to the detonation velocity of the explosive (approximately 7200 m/s). The rapid expansion of the detonation products creates a shock wave with discrete pulse pressure, density, temperature and velocity. The pre and post-shock states are described by conservation equations for mass, momentum and energy, and are referred to as the Rankine–Hugoniot jump equations [18].

The shock wave that travels through the air consists of highly compressed air particles that exert pressure on all surfaces they encounter. There is a discrete ‘‘jump’’ of the shock front pressure, with the pressure rising from ambient (p_a) to p_s . The pressure difference is referred to as the blast overpressure (Fig. 2). At a fixed location in space, the pressure decays exponentially with time and is followed by a negative (suction) phase. An ideal blast wave pressure pulse has a very short time duration, typically measured in fractions of milliseconds. The free-field pressure–time response can be calculated by a modified Friedlander equation [19]:

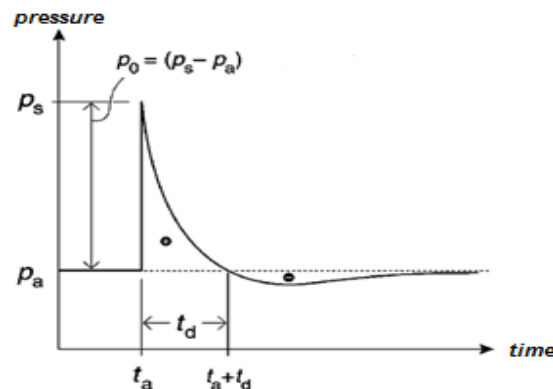


Figure 2. Characteristic air blast pressure response [19]

$$p(t) = (p_s - p_a) \left[1 - \frac{t - t_a}{t_d} \right] e^{-(t-t_a)/\theta} \quad (2)$$

where t_a is the arrival time, t_d the time duration of the positive phase and θ the time decay constant. The air blast load intensity on a target surface depends on the explosive material, the explosive mass (m) and the distance between the explosive and the target (r). The free-field peak pressure of the blast wave (P) for a given explosive is given by:

$$P = K \left(\frac{m}{r^3} \right) \quad (3)$$

where K is an explosive material parameter. When the shock wave encounters a surface, it is reflected, amplifying the incident overpressure. The magnification can be highly non-linear and depends on the incident shock strength and the angle of incidence. For a weak shock, the resultant blast loads are doubled on reflection of the shock wave. For strong shocks, reflection coefficients of 8 have been reported assuming ideal gas conditions and up to 20 when real gas effects such as the dissociation and ionization of air molecules have been considered [18]. The impact load on the structure calculated as:

$$I = \int_{t_a}^{t_a+t_d} p dt \quad (4)$$

where p is the incident pressure multiplied by the pressure reflection coefficient.

3. Numerical simulation and results

One the main methods to evaluate the performance of sandwich panels under dynamic load conditions is air blast test. Nowadays finite element codes allow simulations under these dynamic conditions to be performed without the need for destructive air blast experiments [20, 21]. Three-dimensional dynamic finite element calculations were performed using ABAQUS software [22] to simulate the tests. The sandwich panels were fully meshed using eight-node linear brick elements with reduced integration. Such elements are capable of accurately capturing the stresses and strains. Each face sheet was discretized with five layers of elements through the thickness. The honeycomb core members were meshed using four-node shell elements with finite membrane strains. Five section integration points with Simpson's integration rule were used in each shell element. These elements allow large rotations and membrane deformation, making them particularly well suited for buckling analyses. Thirty layers of elements were uniformly distributed through the core thickness. As shown in Fig. 3, the core webs were "welded" to the face sheet at their connections. Support structures were simply modeled as rigid surfaces and sandwich panels faces were assumed to be welded to the rigid wall at all ends. Figure 4 demonstrates the meshed honeycomb model in ABAQUS.

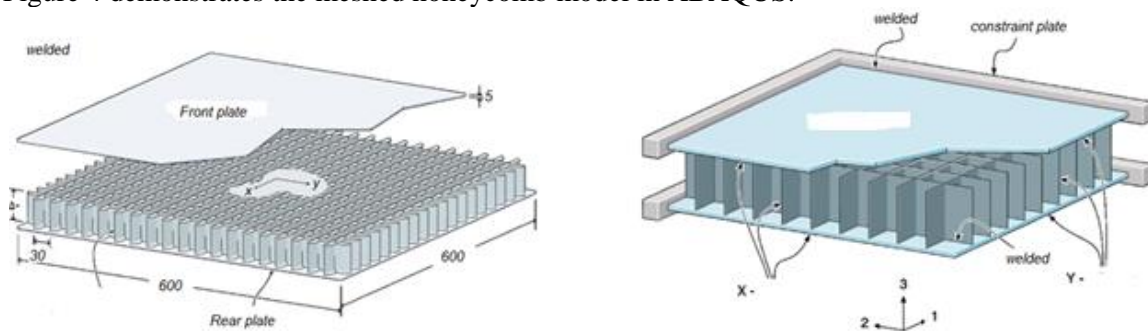


Figure 3. Square honeycomb core sandwich panel design

A failure criterion was not considered in the calculations, so fracture of the plate and core debonding from the front face was not captured. Pressure was applied on the surface of the front face as time varying and spatially distributed functions from calculations made with ConWep for the explosive material, charge weight and standoff distance values used for the test. Although ConWep assumes a spherical air blast (and not a cylindrical charge), it is believed that with center detonated cylindrical charges with length to diameter aspect ratios close to 1, it provides a reasonable estimate of the blast wave pressure loading profile. For any point on the front

surface, its distance to the center of the front face is noted as d , and the pressure on each point can be expressed as:

$$P(d,t)=p(t)e^{-\left(\frac{d}{d_0}\right)^2} \quad (5)$$

where d_0 , is the reference distance, and $p(t)$ is obtained by Eq. (2).

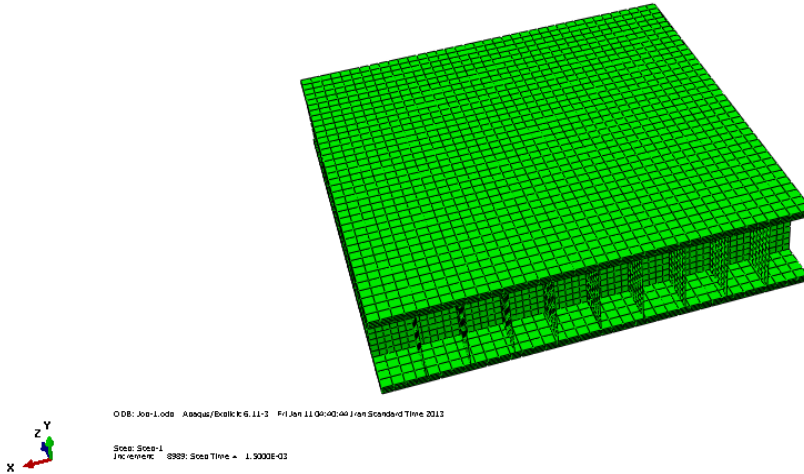


Figure 4. Meshed honeycomb model in ABAQUS

Fig. 5 shows that, when d_0 is set as 0.12 m for all levels of applied impulses, Eq. (5) provides very good estimates of peak pressure on the panel for the whole range of distances. Finally, for simplification and increasing simulation time, due to its symmetry, only one quarter of the panel was analyzed. As shown in fig. 5, the symmetry boundary conditions are applied to the sandwich panel.

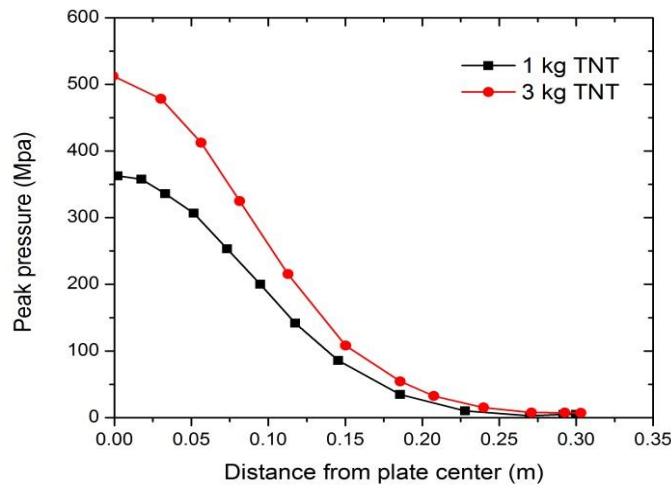


Figure 5. Spatial distributions of peak pressure exerted on the surface from 1 and 3 kg TNT explosions at a 0.1 m distance

Simulations were carried out with strain rate dependence for the stainless steel alloy. This material in its nature has strain hardening which is nearly linear and demonstrates moderate sensitivity to strain rate. In tension, the relation between true stress and true strain is taken to be strictly bilinear for each value of plastic strain rate $\dot{\epsilon}_p$, as:

$$\sigma = \begin{cases} E\varepsilon \rightarrow \varepsilon \leq \frac{\sigma_Y}{E} \left(1 + \left(\frac{\varepsilon_p}{\varepsilon_0}\right)^m\right) \\ \sigma_Y \left(1 + \left(\frac{\varepsilon_p}{\varepsilon_0}\right)^m\right) + E_t \left(\varepsilon - \frac{\sigma_Y}{E} \left(1 + \left(\frac{\varepsilon_p}{\varepsilon_0}\right)^m\right)\right) \rightarrow \varepsilon > \frac{\sigma_Y}{E} \left(1 + \left(\frac{\varepsilon_p}{\varepsilon_0}\right)^m\right) \end{cases} \quad (6)$$

Here, Young’s module $E=200\text{GPa}$, Poisson’s ratio $\nu=0.3$; initial yield stress $\sigma_Y = 300\text{MPa}$ and tangent modulus $E_t = 2.0\text{GPa}$. Dynamic measurements on stainless steels are well represented using the values $\varepsilon_0 = 4916 \text{ s}^{-1}$ and $m=0.154$ [23].

Fig. 8 shows the center deflections of the sandwich panel front face, back face and the equivalent solid plate plotted as a function of the impulse load. The benefits of a sandwich panel construction over a solid plate to withstand blast loads are clearly evident by the lower back plate deflections compared with the equivalent weight solid plates under the same loads. The other advantages of sandwich structures are particularly evident at low impulse levels. Wherein the center deflection of the back face is only about 40% of those for the solid plate. At high impulse values the benefits reduces, the deflections of the sandwich panel being approximately 90% of the solid panel.

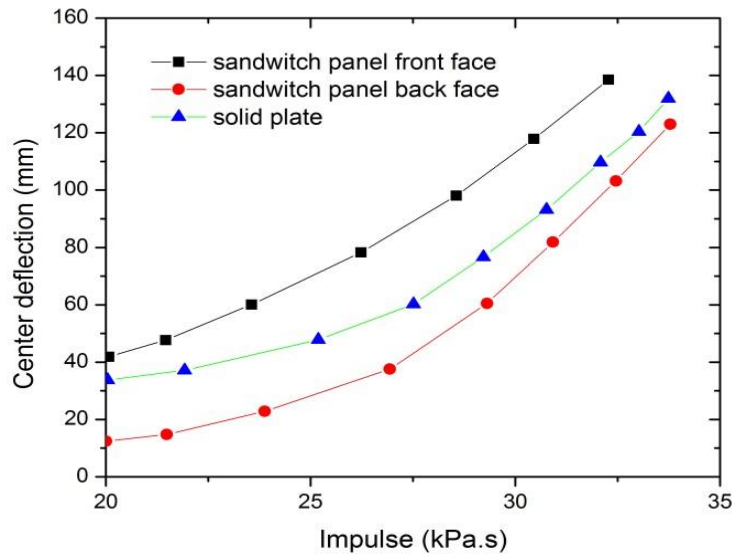


Figure 6. The center deflections of sandwich panel as a function of impulse

Fig. 7 illustrates deformed sandwich panels for each impulse load level predicted by finite element simulations. It is obvious that the simulations capture most of the details of the deformation patterns quite realistically, including shearing of the core and buckling of the lateral webs. The highest intensity load results in a separation between the front face and core webs, so weakening the overall strength of the plate, while the present finite element model does not capture this failure mechanism since a debonding criterion was not included.

Figure 8, illustrates the von mises stress in sandwich panel. When the sandwich panel deforms, the front face starts to stretch very early, then the stretching force remains at a high level, and finally the stretching force is released. While the back face is under compression first, where bending dominates the overall behavior of the sandwich panel, the back face starts to stretch, and finally the stretching force of the back face is also released, which cause earlier fail in the front face.

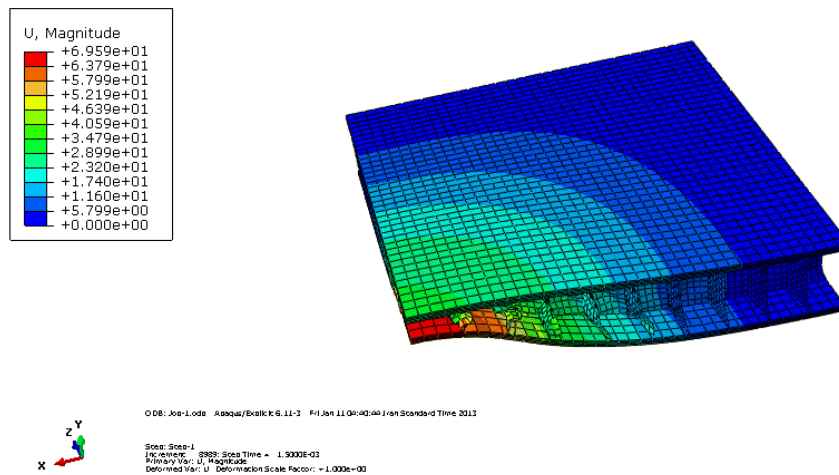


Figure 7. Sandwich panel deformation under 20 Kpa impulse

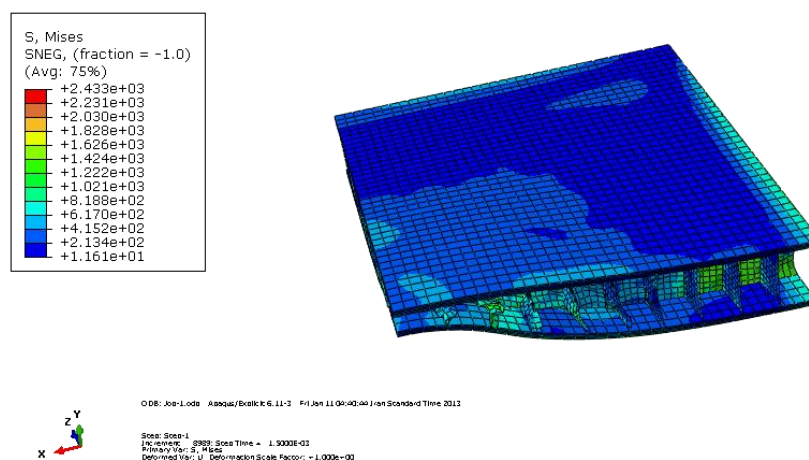


Figure 8. Vonmises stress distribution over sandwich panel deformation under 20 Kpa impulse

Conclusion

In this paper, dynamic mechanical response of sandwich panels with square honeycomb core is carried out using ABAQUS software, which is made of an alloy of stainless steel austenitic. From the series of results obtained in this study, the advantage of using a sandwich structure with a cellular metal core has been demonstrated as a suitable candidate for deflection-limited designs capable of withstanding air blast loads. Finite element simulations carried out on the panels are able to show details of sand which panel deformation is caused by explosive charges. Using of failure criteria in the finite element modeling of the connection between sheet – core and with high intensity explosive loads is necessary.

References

1. Fleck, N.A., Deshpande VS. The resistance of clamped sandwichbeams to shock loading. *Journal of Applied Mechanics* 71 (2004) 386–401.
2. Xue, Z., Hutchinson JW. Preliminary assessment of sandwich platessubject to blast loads. *International Journal of Mechanical Sciences* 45 (2003) 687–705.
3. Xue Z., Hutchinson, J.W. A comparative study of impulse-resistant metal sandwich plates. *International Journal of Impact Engineering* 30 (2004) 1283–305.

4. Rathbun H.J., Radford D.D., Xue Z., He M.Y., Yang J., Deshpande V.S., et al. Performance of metallic honeycomb-core sandwich beams under shock loading. *International Journal of Solids and Structures* 43 (2006) 1746–63.
5. Hutchinson J.W., Xue, Z. Metal sandwich plates optimized for pressure impulses. *International Journal of Mechanical Sciences*, 47 (2005) 545–469.
6. Smith P.D., Hetherington J.G. Blast and ballistic loading of structures. Butterworth-Heinemann: London; (1994).
7. Dharmasena K.P., Wadley, H.N.G., Xue, Z., Hutchinson, J.Y. Mechanical response of metallic honeycomb sandwich panel structures to high-intensity dynamic loading. *International Journal of Impact Engineering* 35 (2008) 1063–1074.
8. Fleck N.A., Deshpande, V.S. The resistance of clamped sandwich beams to shock loading. *Journal of Applied Mechanics* 71 (2004) 386–401.
9. Gibson L.J., Ashby, M.F. Cellular solids: structure and properties. 2nd ed. Cambridge: Cambridge University Press; (1997).
10. Xue Z, Hutchinson J. Crush dynamics of square honeycomb sandwich cores. *International Journal of Numerical Methods in Engineering*, 65 (2005) 2221–45.
11. Karagiozova D., Nurick, G.N., Longdon, G.S. Behaviour of sandwich panels subject to intense air blasts – Part 2: Numerical simulation. *Composite Structures* 91 (2009) 442–450.
12. Chi Y., Longdon G.S., Nurick G.N. The influence of core height and face plate thickness on the response of honeycomb sandwich panels subjected to blast loading, *Materials and Design* 31 (2010) 1887–1899.
13. Wang T., Ma M., Yu W., Dong S., Gao Y. Mechanical Response of Square Honeycomb Sandwich Plate with Asymmetric Face Sheet Subjected to Blast Loading. *Procedia Engineering*, 23 (2011) 457 – 463.
14. Li X., Zhang P., Wang Z., Wu G., Zhao L. Dynamic behavior of aluminum honeycomb sandwich panels under airblast: Experiment and numerical analysis. *Composite Structures*, 108 (2014) 1001–08.
15. Nemat-Nasser S., Guo W.G., Kihl D.P. Thermo mechanical response of AL-6XN stainless steel over a wide range of strain rates and temperatures, *Journal of Mechanics and Physics of Solids* 49 (2001) 23–46.
16. Wadley H.N.G., Fleck N.A., Evans A.G. Fabrication and structural performance of periodic cellular metal sandwich structures. *Composites Science and Technology*, 63 (2003) 31–43.
17. Kooistra G.W., Deshpande, V.S., Wadley, H.N.G. Compressible behavior of age hardenable tetrahedral lattice truss structures made from aluminum. *Acta Materialia*, 52 (2004) 29–37.
18. Baker W.E. Explosions in air. Austin, TX: University of Texas Press; 1973.
19. Uddin N. Blast protection of civil infrastructures and vehicles using composites. Woodhead Publishing Limited, (2010).
20. Chung Kim Yuen S., Nurick, G.N. Experimental and numerical studies on the response of quadrangular stiffened plates. Part I: Subjected to uniform blast load. *International Journal of Impact Engineering* 31(2005) 55–83.
21. Langdon G.S., Chung K.S., Nurick G.N., Experimental and numerical studies on the response of quadrangular stiffened plates. Part II: Localised blast loading. *International Journal of Impact Engineering*, 31 (2005) 85–111.
22. ABAQUS/Explicit user's manual, Version 6.11.
23. Stout M.G., Follansbee P.S. Strain rate sensitivity, strain hardening, and yield behavior of 304L stainless steel. Transactions of ASME: *Journal of Engineering and Materials Technology* 108 (1986) 344–53.

(2015); <http://www.jmaterenvironsci.com>